

# Dip-and-pull ambient pressure photoelectron spectroscopy as a spectroelectrochemistry tool for probing molecular redox processes

Cite as: J. Chem. Phys. **157**, 244701 (2022); <https://doi.org/10.1063/5.0130222>

Submitted: 10 October 2022 • Accepted: 05 December 2022 • Accepted Manuscript Online: 05 December 2022 • Published Online: 22 December 2022

 Robert H. Temperton,  Anurag Kawde,  Axl Eriksson, et al.

## COLLECTIONS

Paper published as part of the special topic on [In situ and Operando Characterization](#)

 This paper was selected as Featured



View Online



Export Citation



CrossMark

## ARTICLES YOU MAY BE INTERESTED IN

[Ultrafast laser spectroscopy uncovers mechanisms of light energy conversion in photosynthesis and sustainable energy materials](#)

Chemical Physics Reviews **3**, 041303 (2022); <https://doi.org/10.1063/5.0092864>

[Time-resolved spectroscopic mapping of vibrational energy flow in proteins: Understanding thermal diffusion at the nanoscale](#)

The Journal of Chemical Physics **157**, 240901 (2022); <https://doi.org/10.1063/5.0116734>

[Electrokinetic, electrochemical, and electrostatic surface potentials of the pristine water liquid-vapor interface](#)

The Journal of Chemical Physics **157**, 240902 (2022); <https://doi.org/10.1063/5.0127869>



The Journal of Chemical Physics **Special Topics** Open for Submissions [Learn More](#)

# Dip-and-pull ambient pressure photoelectron spectroscopy as a spectroelectrochemistry tool for probing molecular redox processes

Cite as: J. Chem. Phys. 157, 244701 (2022); doi: 10.1063/5.0130222

Submitted: 10 October 2022 • Accepted: 5 December 2022 •

Published Online: 22 December 2022 • Publisher Error Corrected: 22 December 2022



View Online



Export Citation



CrossMark

Robert H. Temperton,<sup>1,2,a</sup>  Anurag Kawde,<sup>2,3</sup>  Axl Eriksson,<sup>3</sup>  Weijia Wang,<sup>1</sup>  Esko Kokkonen,<sup>1</sup>   
Rosemary Jones,<sup>4</sup>  Sabrina Maria Gericke,<sup>5</sup>  Suyun Zhu,<sup>1</sup>  Wilson Quevedo,<sup>6</sup>  Robert Seidel,<sup>6,7</sup>   
Joachim Schnadt,<sup>1,2,4</sup>  Andrey Shavorskiy,<sup>1</sup>  Petter Persson,<sup>2,8</sup>  and Jens Uhlig<sup>2,3</sup> 

## AFFILIATIONS

<sup>1</sup>MAX IV Laboratory, Lund University, Box 118, 221 00 Lund, Sweden

<sup>2</sup>Lund Institute of Advanced Neutron and X-ray Science, IDEON Building: Delta 5, Scheelevägen 19, 223 70 Lund, Sweden

<sup>3</sup>Division of Chemical Physics, Department of Chemistry, Lund University, Box 124, 221 00 Lund, Sweden

<sup>4</sup>Division of Synchrotron Radiation Research, Department of Physics, Lund University, Box 118, 22 100 Lund, Sweden

<sup>5</sup>Division of Combustion Physics, Faculty of Engineering, Lund University, Box 118, 22 100 Lund, Sweden

<sup>6</sup>Helmholtz-Zentrum Berlin für Materialien und Energie, Albert-Einstein-Strasse 15, 12489 Berlin, Germany

<sup>7</sup>Department of Chemistry, Humboldt-Universität zu Berlin, Brook-Taylor-Straße 2, D-12489 Berlin, Germany

<sup>8</sup>Division of Theoretical Chemistry, Department of Chemistry, Lund University, Box 124, 221 00 Lund, Sweden

**Note:** This paper is part of the JCP Special Topic on In situ and Operando Characterization.

<sup>a</sup>**Author to whom correspondence should be addressed:** [robert.temperton@maxiv.lu.se](mailto:robert.temperton@maxiv.lu.se)

## ABSTRACT

Ambient pressure x-ray photoelectron spectroscopy (APXPS) can provide a compelling platform for studying an analyte's oxidation and reduction reactions in solutions. This paper presents proof-of-principle *operando* measurements of a model organometallic complex, iron hexacyanide, in an aqueous solution using the dip-and-pull technique. The data demonstrates that the electrochemically active liquid menisci on the working electrodes can undergo controlled redox reactions which were observed using APXPS. A detailed discussion of several critical experimental considerations is included as guidance for anyone undertaking comparable experiments.

© 2022 Author(s). All article content, except where otherwise noted, is licensed under a Creative Commons Attribution (CC BY) license (<http://creativecommons.org/licenses/by/4.0/>). <https://doi.org/10.1063/5.0130222>

## I. INTRODUCTION

The capability of performing photoelectron spectroscopy (PES) measurements of a sample under electrochemical control has been realized by several approaches to electrochemical cell design, each with competing advantages and disadvantages.<sup>1</sup> The dip-and-pull method<sup>2</sup> is becoming an increasingly used approach, with instruments now available at numerous synchrotron radiation facilities.<sup>2–5</sup> It has also been demonstrated recently using an x-ray anode source.<sup>6</sup> The typical objective for dip-and-pull experiments has been to probe electrochemically controlled solid–liquid interfaces, for which ambient pressure x-ray photoelectron spectroscopy (APXPS) can provide

insight into the interfacial chemistry.<sup>7</sup> Some studies have focused on the liquid film itself, where kinetic energy shifts have been used to infer information about the electrochemical double layer,<sup>8</sup> band alignment,<sup>9</sup> and charge transfer reactions.<sup>10,11</sup> There have, however, been no papers using dip-and-pull APXPS to study the electrochemical properties of a complex analyte in solution.

More generally, spectroelectrochemical techniques are powerful for researching charge transfer processes where properties such as oxidation state and electronic structure are critical.<sup>12,13</sup> One application of spectroelectrochemistry has been the development of efficient organometallic complexes for a range of photofunctional applications, including light harvesting.<sup>13</sup> The capabilities of

PES for the characterization of photofunctional complexes has been repeatedly demonstrated, for example as a probe of surface chemistry, electronic structure, and charge transfer.<sup>14–20</sup> Applying PES to electrochemically induced oxidation state changes could elucidate critical processes that underpin the functionality of a complex in molecular devices.

This paper presents a proof-of-principle study demonstrating the feasibility of studying molecular redox processes using dip-and-pull APXPS. We achieved this through *operando* PES measurements of an aqueous solution of the model complex  $[\text{Fe}^{\text{III}}(\text{CN})_6]^{3-}$  (iron-III hexacyanide). While using water as the solvent poses several experimental challenges, which we discuss later, the ubiquity of water makes it ideally suited for a proof-of-principle experiment. Iron hexacyanide was selected as it is a commercially available, low-cost, and well-studied complex that has been previously measured using PES in both aqueous solution<sup>21,22</sup> and in the solid/crystalline form.<sup>23,24</sup> This complex's electrochemistry is well understood, and it can be repeatedly cycled between the  $\text{Fe}^{\text{II}}$  and  $\text{Fe}^{\text{III}}$  oxidation states, as has been studied with *operando* x-ray absorption spectroscopy.<sup>25</sup> We additionally include a detailed discussion of several experimental considerations that will be of value to anyone wanting to use APXPS as a spectroelectrochemical method.

## II. METHODS

Spectroelectrochemistry measurements were carried out at the MAX IV Laboratory using the electrochemistry cell at the HIPPIE beamline.<sup>4</sup> This is equipped with a Scienta HIPPIE-3 analyzer (with a  $\sim 0.15$  mm diameter entrance cone) positioned in the horizontal plane at  $55^\circ$  from the x-ray beam (set to linear-horizontal polarization). A photon energy of 1420 eV was used. The projected x-ray spot size on the sample is  $\sim 100 \times 25 \mu\text{m}^2$  (horizontal  $\times$  vertical). The overall photoelectron kinetic energy resolution of measurements is estimated to be  $\sim 0.5$  eV.

The working electrode was a 7 nm film of TiN, grown by atomic layer deposition on fluorine-doped tin oxide (FTO) coated glass, which was found to be electrochemically and mechanically stable. It was positioned  $\sim 0.3$  mm from the analyzer cone at normal emission. The counter electrode was a 0.3 mm diameter Pt wire and the reference electrode was a leakless Ag/AgCl (eDAQ ET072). All three electrodes were held on a manipulator from the top of the chamber. A beaker containing a 0.2 M aqueous solution of  $\text{K}_3\text{Fe}(\text{CN})_6$  (from Sigma-Aldrich) was supported on another manipulator from the bottom of the chamber. The beaker holder was cooled slightly to  $\sim 15^\circ\text{C}$ , reducing the vapor pressure of the solution such that the equalized chamber pressure was  $\sim 17$  mbar after pumping down. The solution was thoroughly degassed in a separate chamber prior to use.

The dip-and-pull technique<sup>2</sup> was used to create a thin film of electrolyte solution on the surface of the working electrode. This liquid film was then studied using PES. A scheme of the setup is included in Fig. 1. First, the electrodes were dipped into the beaker of electrolyte solution, which was positioned just below the entrance to the analyzer. The electrodes were then pulled out of the beaker, producing a thin and electrochemically active liquid film at the measurement position. The three electrodes were in permanent electrical contact with the solution in the beaker, with the relative potentials controlled by a Biologic SP-200 potentiostat. The working electrode

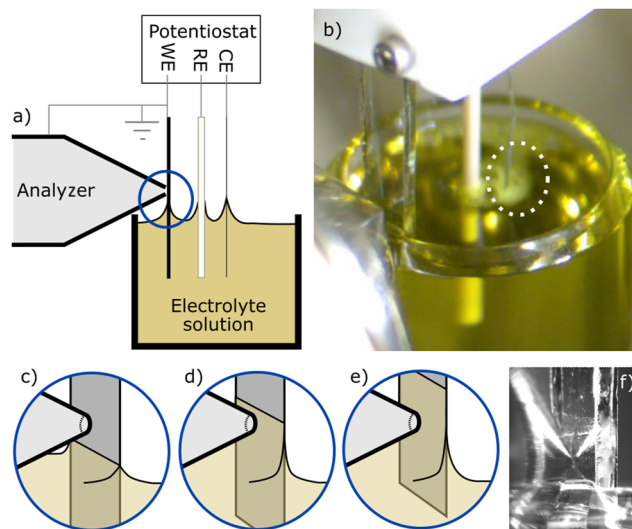


**FIG. 1.** (a) Scheme of the dip-and-pull setup, where WE, RE, and CE are the working, reference, and counter electrodes, respectively. (b) Photograph of the setup. The white dashed circle highlights the evolution of a mist of small hydrogen bubbles at the counter electrode. (c)–(e) Scheme of the dip-and-pull process. The electrodes are first “dipped” [position (c)] before being “pulled” up, with measurements taken while slowly moving between positions shown in (d) and (e). (f) A photograph of the working electrode in the measurement position.

was grounded together with the hemispherical analyzer to allow PES measurements. Therefore, an applied working electrode potential,  $E_{WE}$ , represents the potential difference between the working electrode and the reference electrode, the latter of which is controlled by the potentiostat relative to the external ground. Setting the potentiostat to increase  $E_{WE}$  therefore increased the electrochemical potential of the liquid, causing the photoelectron spectra of the liquid to shift toward higher kinetic energy. Theoretically, assuming no charge transfer, electrochemical reactions, or voltage losses, the kinetic energy shift of the bulk liquid should be 1 eV per 1 V of applied potential. Detailed discussion of how the liquid electrochemical potential impacts photoelectron kinetic energies in this dip-and-pull configuration can be found elsewhere.<sup>8,10</sup> Unless explicitly stated, the applied working electrode potential,  $E_{WE}$ , is given vs the Ag/AgCl reference.

Beam damage was avoided by continually moving the sample during measurements (the sample was continually pulled upward at a velocity of  $0.02 \text{ mm s}^{-1}$ ). Given the vertical spot size at HIPPIE of  $\sim 25 \mu\text{m}$ , each position on the sample was therefore exposed to the x-ray beam for  $\sim 1$  s. This velocity was determined from a series of fast measurements (using the snapshot mode of the hemispherical analyzer) of the  $\text{Fe } t_{2g}$  derived highest occupied molecular orbital (HOMO) using resonant photoelectron spectroscopy, which has been well characterized for both  $[\text{Fe}^{\text{II}}(\text{CN})_6]^{4-}$  and  $[\text{Fe}^{\text{III}}(\text{CN})_6]^{3-}$  solutions and is a clear indicator of the complex's electronic structure.<sup>21</sup> Radiation damage was observed via a kinetic energy shift of the HOMO feature and a subsequent disappearance of the HOMO signal. This happened when the same portion of the

sample was exposed to the x-ray beam for over one second. Our sample movement entirely mitigated this damage.

Liquid-jet measurements were carried out with the SOL<sup>3</sup>PES experimental station<sup>26</sup> at the U49/2-PGM-1 beamline<sup>27</sup> at the BESSY II synchrotron radiation facility. The Scienta HIPPI-2 hemispherical analyzer angle was set at 54.7° relative to the linear-horizontal polarization axis of the x-ray beam. A photon energy of 1270 eV was used. The overall kinetic energy resolution was estimated to be ~0.5 eV. For the liquid-jet experiments, K<sub>3</sub>Fe(CN)<sub>6</sub> and K<sub>4</sub>Fe(CN)<sub>6</sub> (from Sigma-Aldrich) were dissolved in de-ionized water to concentrations of 0.3 and 0.4 M, respectively. These solutions were degassed using an ultrasonic bath and then supplied using a high-performance liquid chromatography (HPLC) pump through a fused silica capillary (30 μm inner diameter), forming a liquid microjet. We cooled the jet assembly to 10 °C to reduce the water vapor pressure in the chamber. Measurements were conducted ~1 mm downstream of the jet nozzle, which was at a distance of 0.5 mm from the analyzer entrance (a 0.5 mm diameter orifice). The pressure in the vacuum chamber during the measurements was better than  $2 \times 10^{-4}$  mbar, which was achieved by a combination of cold traps and a turbomolecular pump.

For the liquid-jet measurements, the relative calibration of the kinetic energy scale was confirmed using the O 1s spectra originating from the water solvent (no shift had to be applied). For the dip-and-pull measurements, the kinetic energies presented are as measured by the analyzer with no offset applied. A raw kinetic energy scale is chosen over a more traditional binding energy scale because binding energy values, calculated from the difference between photon energy and kinetic energy, loose meaning when voltages are applied to the electrochemical cell, causing the photoelectron kinetic energies to shift in response. A detailed discussion of the possible kinetic energy shifts for a gas–liquid–semiconductor system can be found elsewhere.<sup>28</sup> Peak fitting was done using a linear background and Voigt functions with the Lorentzian width fixed to 0.4 eV. Other parameters were allowed to vary. The full fits are included in the [supplementary material](#), whereas only the highest kinetic energy components are included in the manuscript as an indicator of spectral shifts (the multiplet structures are not relevant to this discussion).

### III. RESULTS

This paper uses Fe 2*p* PES to demonstrate the switching of iron hexacyanide between the Fe<sup>II</sup> and Fe<sup>III</sup> oxidation states. [Figure 2](#) presents the Fe 2*p* PES of the chemically generated [Fe<sup>II</sup>(CN)<sub>6</sub>]<sup>4-</sup> and [Fe<sup>III</sup>(CN)<sub>6</sub>]<sup>3-</sup> dissolved in water, measured using a liquid microjet. These provide radiation-damage-free references of the spectral shape of the complexes in the Fe<sup>II</sup> and Fe<sup>III</sup> oxidation states. In both cases, the Fe 2*p*<sub>3/2</sub> (between 550 and 560 eV kinetic energy) and Fe 2*p*<sub>1/2</sub> (between 540 and 545 eV kinetic energy) spin–orbit components are shown, with no obvious other structures observable within the noise level. For [Fe<sup>II</sup>(CN)<sub>6</sub>]<sup>4-</sup>, the Fe 2*p*<sub>3/2</sub> feature resembles a single peak, whereas the Fe<sup>III</sup> spectrum shows a multiplet structure with a clear shoulder on the lower kinetic energy side of the peak. These line shapes are similar to Fe 2*p* PES measurements of the solid/crystalline powder form as K<sub>3</sub>Fe(CN)<sub>6</sub>.<sup>23,24</sup> However, we observe a larger shift of ~1.9 eV between the two main Fe 2*p*<sub>3/2</sub> peaks

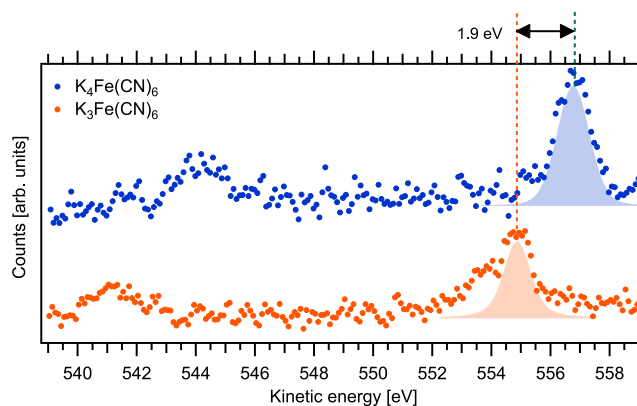


**FIG. 2.** Liquid microjet, Fe 2*p*, PES measurements of aqueous solutions of K<sub>4</sub>Fe(CN)<sub>6</sub> (top, blue spectrum) and K<sub>3</sub>Fe(CN)<sub>6</sub> (bottom, orange spectrum). These provide reference spectra of the iron hexacyanide complex in the Fe<sup>II</sup> and Fe<sup>III</sup> oxidation states, collected with 1270 eV excitation energy. The solid peaks correspond to the highest kinetic energy component from peak fitting.

in the liquid-jet measurements in contrast to ~1.2 eV as reported for solid samples.<sup>23,24</sup>

A cyclic voltammogram of K<sub>3</sub>Fe(CN)<sub>6</sub>, measured *in situ* (using the dip-and-pull configuration) prior to the PES measurements, is presented in [Fig. 3\(b\)](#). The two cycles, measured at a scan rate of 100 mV s<sup>-1</sup>, are shown over the selected potential range between -1 and 1 V, which covers both the reduction and oxidation peaks. The 1.4 eV splitting between the reduction and oxidation potentials is consistent with other measurements at this scan rate.<sup>29</sup> The apparent linear background in the cyclic voltammogram is likely caused by sizable ohmic currents, the relatively high scan rate and large ~2 cm distance between working and counter electrodes. It is

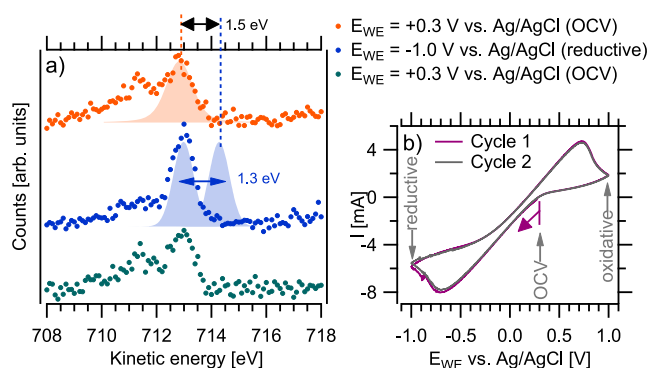


**FIG. 3.** (a) Fe 2*p* spectra of an aqueous solution of K<sub>3</sub>Fe(CN)<sub>6</sub> using the dip-and-pull method measured before (top, orange), during (middle, blue), and after (bottom, green) a reductive potential hold of -1 V. For each spectrum, the electrodes were dipped and pulled to refresh the sample. The solid peaks show the highest kinetic energy component from peak fitting. For the blue spectra at the reductive potential, the peak is additionally shown to be shifted by 1.3 eV in accordance with the applied potential. The photon energy was 1420 eV. (b) Cyclic voltammogram of the K<sub>3</sub>Fe(CN)<sub>6</sub> solution immediately prior to the PES measurements, starting at OCV and first sweeping in the reductive direction. The first two cycles are shown.

worth noting that in this experiment, no buffers were used to stabilize the pH of the solution. We thus observed potential drift over time (offline tests of a significantly smaller volume of similar solution showed a change from pH7 to approximately pH10 after 15 cyclic voltammogram cycles). However, the presented cyclic voltammogram was measured immediately prior to the presented PES measurements and the potentials are therefore representative. The open circuit voltage (OCV) of the working electrode was measured to be  $\sim 0.3$  V vs the Ag/AgCl reference electrode throughout the presented experiments.

Figure 3(a) shows Fe  $2p_{3/2}$  PES measurements of a liquid film produced by the dip-and-pull method, first with the cell under open circuit conditions (orange spectrum), then with the working electrode held at a reduction potential of  $E_{WE} = -1$  V vs the Ag/AgCl reference electrode (blue spectrum) and finally a repeat measurement under open circuit conditions (green spectrum). Between each measurement, the electrodes were redipped into the electrolyte refreshing the liquid film on the electrode. The same dip-and-pull motions and velocities were used for all three measurements to ensure repeatability of the liquid film and the measurements were taken over the same area of the electrode surface. Each spectrum represents a cumulative measurement time of  $\sim 75$  s. The two spectra measured at OCV in Fig. 3 are similar in shape to the  $[\text{Fe}^{\text{III}}(\text{CN})_6]^{3-}$  spectra in Fig. 2, which can be expected due to the natural  $\text{Fe}^{\text{III}}$  oxidation state of the complex in  $\text{K}_3\text{Fe}(\text{CN})_6$ . The middle spectra measured with an applied reductive potential of  $E_{WE} = -1$  V vs Ag/AgCl is similar to the  $[\text{Fe}^{\text{II}}(\text{CN})_6]^{4-}$  reference spectra, demonstrating that we are able to successfully change the oxidation state of the complex from  $\text{Fe}^{\text{III}}$  to  $\text{Fe}^{\text{II}}$ .

The working electrode OCV of 0.3 V and an applied potential of  $E_{WE} = -1$  V, both relative to the Ag/AgCl reference electrode, implies a  $\sim 1.3$  V difference in the electrochemical potential of the liquid with and without the applied potential. One would expect this difference in electrochemical potential to manifest in the spectra as a proportionate kinetic energy shift, assuming a minimal potential drop between the bulk liquid (for which the electrochemical measurements are representative) and the liquid film (which we are measuring). In Fig. 3, the main component of the reduced  $\text{Fe}^{\text{II}}$  spectrum (blue filled peak obtained from peak fitting) is therefore also shown to be shifted by 1.3 eV to facilitate comparison with the  $\text{Fe}^{\text{III}}$  spectrum. This implies a  $\sim 1.5$  eV offset between the center of main  $\text{Fe}^{\text{II}}$  and  $\text{Fe}^{\text{III}}$  peaks, which is  $\sim 0.4$  eV smaller than the liquid-jet measurements in Fig. 2.

Figure 4 shows an *operando* experiment during a single “pull” of the electrodes from the electrolyte solution. The three traces represent consecutive PES measurements/sweeps, each with a duration of  $\sim 25$  s. The first PES sweep was under the reductive potential hold condition of  $E_{WE} = -1$  V vs Ag/AgCl, which is consistent with the previous *in situ* measurement. During sweep 2, a voltage sweep was applied, changing the potential difference between the working and reference electrodes to the oxidative potential of 1 V vs Ag/AgCl, where the potential was held during sweep 3. In sweep 2, where the potential was changing during the measurement, the shift of the peak toward higher kinetic energies is consistent with the direction of the voltage sweep with no change in shape. We tentatively interpret it to represent a shift in the solution’s electrochemical potential without any change in the oxidation state. However, we would like to stress that the precise electrochemical conditions at the time

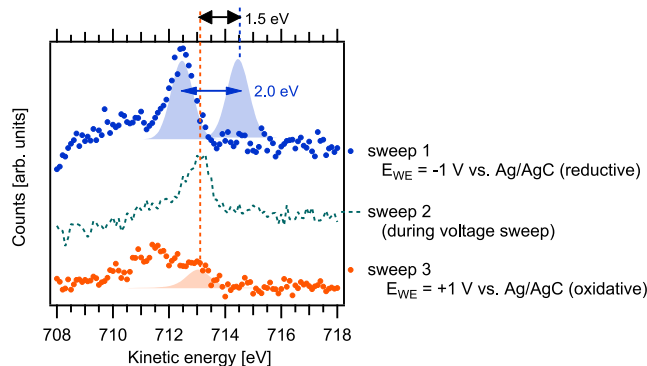


FIG. 4. Consecutive Fe  $2p$  PES measurements/sweeps on the  $\text{K}_3\text{Fe}(\text{CN})_6$  solution during a single “pull.” The working electrode was initially at a reductive potential of  $-1$  V. During the second measurement/sweep, the voltage was changed to the oxidizing potential of  $+1$  V and held there for the final sweep. The solid peaks show the highest kinetic energy component from peak fitting. For the blue spectra at the reductive potential, the peak is additionally shown to be shifted by 2 eV to compensate for the difference in applied potential. The photon energy was 1420 eV.

when the photoelectron peak was acquired are not known and that definitive conclusions should not be drawn from this spectrum. The discussion will therefore focus on spectral changes between sweeps 1 and 3.

Again comparing the spectra in Fig. 4 to the reference spectra in Fig. 2, sweep 1 looks like the single peak attributed to  $\text{Fe}^{\text{II}}$ , while the broader structure in sweep 3 is more like the  $\text{Fe}^{\text{III}}$  line shape. We do however note that in the latter case, the intensity ratios of the multiplet structure do not appear to be correct (see the discussion section). We additionally note that broadening of the liquid’s photoemission peaks can arise in this dip-and-pull geometry, especially when the electrode is moving during measurement and the potential is changing. The probing volume is therefore ill defined relative to the electrode surface, which can affect the electrostatics and thus spectral shape.<sup>8</sup>

In this experimental configuration, the measured region of the liquid film was  $\sim 3$  mm above the bulk liquid in the beaker. While the working electrode and the electron analyzer are kept at the same absolute potential (they share the same ground), the change in kinetic energy from the electrons originating from the solvated molecules shows that the relative potential of measured liquid meniscus is electrochemically active. This also means that the relative potential between the liquid and the working electrode is adapting fast and we can treat the interaction as in a normal electrochemical cell. While these data have a worse signal-to-noise ratio than Fig. 3 (each spectrum here was collected in one-third of the time), Fig. 4 shows that after reducing the molecule, we are able to re-oxidize it and thus perform *operando* measurements of the process without refreshing the liquid.

Sweep 1 was measured at  $E_{WE} = -1$  V and sweep 3 at  $E_{WE} = 1$  V, both relative to the same Ag/AgCl reference, representing a 2 V difference in the applied potential. We can again attempt to compensate for this difference by shifting the reduced (blue) peak relative to the oxidized (orange) spectrum by 2 eV (as labeled in Fig. 4). This implies a kinetic energy offset of  $\sim 1.5$  eV between the

main Fe<sup>II</sup> and Fe<sup>III</sup> components, the same offset as was observed in Fig. 3 dataset.

The above dip-and-pull measurements were repeatable.

#### IV. DISCUSSION

The interpretation of electrochemical PES data is nuanced and requires careful consideration. First, we note that the absolute binding energy position of the peaks cannot be used as a reference. For dip-and-pull measurements of liquids, it is well understood that while the working electrode is grounded to the analyzer, the liquid film is not necessarily at the same potential. This is because in this electrochemical configuration, the potentiostat controls the potential of the bulk liquid relative to the working electrode. However, a change in the applied potential does not necessarily result in an equal kinetic energy shift in PES measurements of the liquid. A simple example of particular relevance to dip-and-pull is ohmic  $iR$  drop up the thin liquid meniscus due to insufficient ion transport. Other examples include the influence of electrochemical double layer and charge transfer reactions.<sup>8,10</sup> It is also worth noting that we are using the word “potential” empirically in this context, mainly based on the observed shifts in spectra and the potential differences applied/measured by the potentiostat. Physically, however, there are many types of potentials relevant to the interfaces between the electrode, the electrolyte solution, and gaseous environment where the electrode potential, chemical potential, electric potential, and electrochemical potential formally have very different definitions.<sup>30</sup> A helpful guide of how various types of potential can be combined with APXPS can be found in the thesis of Källquist.<sup>31</sup>

With regard to the kinetic energy shifts we observed between  $[\text{Fe}^{\text{II}}(\text{CN})_6]^{4-}$  and  $[\text{Fe}^{\text{III}}(\text{CN})_6]^{3-}$  ( $\Delta KE$ ), we note that the liquid-jet measurements of the chemically induced Fe<sup>II</sup> and Fe<sup>III</sup> species ( $\Delta KE = 1.9$  eV) do not match the existing measurements in the solid phase ( $\Delta KE = 1.2$  eV).<sup>23,24</sup> With regard to spectroelectrochemical measurements, the two experiments give  $\Delta KE \sim 1.5$  eV after accounting for the difference in applied potentials. The difference in applied potential was different for these two spectroelectrochemical experiments, yet  $\Delta KE$  remained the same. There was therefore minimal ohmic  $iR$  drop up the meniscus/liquid film. This supports the conclusion that the measured liquid was electrochemically active. As such, the system behaved like a standard electrochemical cell where, to a reasonable approximation, only the potential difference between the working and reference electrode needed to be considered. The variation in  $\Delta KE$  for the different forms/sample-environments (solid crystal, solvated thin film and liquid-jet) likely originates from screening effects due to different electrostatic and/or chemical environments around the central iron atom. This however warrants further investigation.

The experiment presented a serious challenge of unwanted hydrogen evolution reactions, which in low pressure environments produced violent bubbling. This was even problematic when the applied working electrode potential (relative to Ag/AgCl) was within the operational electrochemical window of water. This is because under oxidizing working electrode potentials, the compliance potential on the counter electrode would far exceed the onset potential for hydrogen evolution (in order to sustain current flow through the circuit). This problem was exacerbated by the high conductivity of the

solution, which is unavoidable in order to have a sufficiently high concentration of the analyte for practical measurement times. The evolution of hydrogen bubbles disrupted the stability of the liquid surface during measurement and impacted the spectral shape, even when they were only produced at the counter electrode. We suspect this is why the spectrum in Fig. 4, where we operated the cell with the working electrode at an oxidizing potential, has an inconsistent shape. The bubbling was minimized by using only a thin wire as counter electrode, which resulted in smaller and more manageable bubbles [visible in Fig. 1(b) as a light mist around the counter electrode, indicated with a dashed circle]. However, its smaller surface area can result in the potentiostat generating higher compliance voltages to maintain a current-free reference electrode. Balancing all of these factors requires careful consideration.

The evolution of hydrogen also caused the pH of the unbuffered solution to change, thus impacting the electrochemical potentials. To our knowledge, there has been no systematic investigation of the impact of pH on the photoelectron spectra of a complex analyte in solution. There are examples where spectral shifts have been measured when pH differences induce a substantial chemical change. This includes the conversion between an anion, zwitterion, and cation, where the spectral effect is largely localized to the atoms at which the charge is changed.<sup>32</sup> For the case of iron hexacyanide presented in this paper, any pH effect would be substantially more minor and we would therefore not expect changes in pH to have a notable impact on the kinetic energies of the Fe  $2p$  photoelectrons (especially given the energy resolution of  $\sim 0.5$  eV). The electrostatic environment of the Fe  $2p$  electrons is likely dominated by the formal oxidation state of the Fe atom and its highly covalent interaction with the cyanide ligands that produce a strong ligand-field.

We successfully mitigated radiation damage by constantly moving (“pulling”) the sample during measurements. The requirement for high x-ray flux, which makes radiation damage such an issue, originates from factors including the desire for fast acquisitions for *operando* measurements and compensating for the scattering the photoelectrons by the gas phase water molecules. The latter is significant at the relatively high ambient pressure of  $\sim 17$  mbar. Continually moving the sample during measurements does require the use of a very flat and straight working electrode in order to remain in the focal spot of the analyzer and the incident x-ray beam. We would like to emphasize that the high probability of radiation damage, especially at modern beamlines on 4th generation light sources, cannot be overlooked. For these fragile complexes, it can manifest strongly within a single second of exposure. Thus, without very fast measurements and a robust strategy for assessing the damage, it could easily be missed and distort the results.

The issue of hydrogen production that we attributed to the use of water as solvent could be aided by using other electrodes or by instead using an organic solvent with a wider electrochemical window. Lower vapor pressure solvents, in the low or sub-mbar range, would additionally allow the beamline to be operated at a significantly lower flux. Solvents such as propylene carbonate<sup>10,11</sup> and 3-methoxypropionitrile meet these requirements and both work well with dip-and-pull experiments.

Future developments will target the use of smaller quantities of liquid in the milliliter range. This will allow the study of more precious analytes by using the dip-and-pull method instead of the more demanding flow cells or liquid microjets that typically require larger

volumes of liquid. Characterization using “soft” x rays, in contrast to the “tender” photon energies more commonly used for dip-and-pull experiments, allows access to many transition metal L-edges for x-ray absorption spectroscopy and/or resonant PES. Such experiments would allow for an electronic structure analysis of solvated analytes in exotic oxidation states that are not stable if produced *ex situ*. Such studies could include the experimental validation of theoretically predicted intermediates in electrochemical reactions.

## V. CONCLUSIONS

We have demonstrated that it is viable to use dip-and-pull APXPS for studying molecular redox processes in metal-organic complexes using the model system of  $K_3Fe(CN)_6$  in aqueous solution. Under static potential conditions, we evidenced the conversion of the  $[Fe^{III}(CN)_6]^{3-}$  analyte into  $[Fe^{II}(CN)_6]^{4-}$  and performed *in situ* characterization of the metal center. *Operando* measurements show that we reverse this change back into the  $Fe^{III}$  form, highlighting that the film of liquid on the electrode is electrochemically active such that the relative potential difference between the working electrode and the solution can be controlled to a large extent. However, measurements of this type are experimentally challenging, and we tried to highlight many of the practical considerations necessary as a useful guide for users of this emerging and exciting type of spectroelectrochemical characterization.

## SUPPLEMENTARY MATERIAL

The full peak fitting of the spectra is included in the [supplementary material](#).

## ACKNOWLEDGMENTS

We acknowledge the MAX IV Laboratory for time on the HIPPIE beamline under Proposal 20210269. Research conducted at MAX IV, a Swedish national user facility, is supported by Vetenskapsrådet (VR, the Swedish Research Council) under Contract No. 2018-07152, the Swedish Governmental Agency for Innovation Systems (VINNOVA) under Contract No. 2018-04969, and Formas under Contract No. 2019-02496.

We acknowledge the Helmholtz-Zentrum Berlin (H.Z.B.) and the staff at BESSY II for generously supporting our measurements.

We gratefully acknowledge financial support from VR and the Knut and Alice Wallenberg Foundation (KAW). R.H.T. and A.K. acknowledge postdoc funding from Lund University. R.S. and W.Q. acknowledge funding from the Deutsche Forschungsgemeinschaft (DFG, German Research Foundation) through an Emmy-Noether grant (SE 2253/3-1). J.U. acknowledges funding from the Crafoordska stiftelsen and the VR under Contract No. 2020-04995. P.P. acknowledges VR for financial support (Grant No. 2021-05313). S.M.G. acknowledges funding from the Swedish Foundation for Strategic Research (Project No. ITM17-0045).

## AUTHOR DECLARATIONS

### Conflict of Interest

The authors have no conflicts to disclose.

## Author Contributions

**Robert H. Temperton:** Conceptualization (lead); Formal analysis (lead); Investigation (lead); Methodology (lead); Project administration (equal); Visualization (lead); Writing – original draft (lead); Writing – review & editing (lead). **Anurag Kawde:** Investigation (equal); Writing – review & editing (equal). **Axl Eriksson:** Investigation (equal); Writing – review & editing (supporting). **Weijia Wang:** Investigation (equal). **Esko Kokkonen:** Investigation (equal); Writing – review & editing (supporting). **Rosemary Jones:** Investigation (equal); Writing – review & editing (supporting). **Sabrina Maria Gericke:** Investigation (equal); Writing – review & editing (supporting). **Suyun Zhu:** Methodology (equal). **Wilson Quevedo:** Investigation (equal); Writing – review & editing (supporting). **Robert Seidel:** Investigation (equal); Writing – review & editing (equal). **Joachim Schnadt:** Writing – review & editing (equal). **Andrey Shavorskiy:** Methodology (equal); Writing – review & editing (equal). **Petter Persson:** Investigation (equal); Project administration (equal); Writing – review & editing (equal). **Jens Uhlig:** Conceptualization (equal); Investigation (equal); Project administration (equal); Writing – review & editing (lead).

## DATA AVAILABILITY

The data that support the findings of this study are available from the corresponding author upon reasonable request.

## REFERENCES

- 1 J.-J. Velasco-Vélez, L. J. Falling, D. Bernsmeier, M. J. Sear, P. C. J. Clark, T.-S. Chan, E. Stotz, M. Hävecker, R. Kraehnert, A. Knop-Gericke, C.-H. Chuang, D. E. Starr, M. Favaro, and R. V. Mom, “A comparative study of electrochemical cells for *in situ* x-ray spectroscopies in the soft and tender x-ray range,” *J. Phys. D: Appl. Phys.* **54**, 124003 (2021).
- 2 S. Axnanda, E. J. Crumlin, B. Mao, S. Rani, R. Chang, P. G. Karlsson, M. O. M. Edwards, M. Lundqvist, R. Moberg, P. Ross, Z. Hussain, and Z. Liu, “Using “tender” x-ray ambient pressure x-ray photoelectron spectroscopy as a direct probe of solid-liquid interface,” *Sci. Rep.* **5**, 9788 (2015).
- 3 Z. Novotny, D. Aegerter, N. Comini, B. Tobler, L. Artiglia, U. Maier, T. Moehl, E. Fabbri, T. Huthwelker, T. J. Schmidt, M. Ammann, J. A. Van Bokhoven, J. Raabe, and J. Osterwalder, “Probing the solid-liquid interface with tender x rays: A new ambient-pressure x-ray photoelectron spectroscopy endstation at the Swiss light source,” *Rev. Sci. Instrum.* **91**, 023103 (2020).
- 4 S. Zhu, M. Scardamaglia, J. Kundsén, R. Sankari, H. Tarawneh, R. Temperton, L. Pickworth, F. Cavalca, C. Wang, H. Tissot, J. Weissenrieder, B. Hagman, J. Gustafson, S. Kaya, F. Lindgren, I. Källquist, J. Maibach, M. Hahlin, V. Boix, T. Gallo, F. Rehman, G. D’Acunto, J. Schnadt, and A. Shavorskiy, “HIPPIE: A new platform for ambient-pressure x-ray photoelectron spectroscopy at the MAX IV laboratory,” *J. Synchrotron Radiat.* **28**, 624–636 (2021).
- 5 M. Favaro, P. C. J. Clark, M. J. Sear, M. Johansson, S. Maehl, R. van de Krol, and D. E. Starr, “Spectroscopic analysis with tender x-rays: SpAnTeX, a new AP-HAXPES end-station at BESSY II,” *Surf. Sci.* **713**, 121903 (2021).
- 6 C. Liu, Q. Dong, Y. Han, Y. Zang, H. Zhang, X. Xie, Y. Yu, and Z. Liu, “Understanding fundamentals of electrochemical reactions with tender X-rays: A new lab-based *operando* x-ray photoelectron spectroscopy method for probing liquid/solid and gas/solid interfaces across a variety of electrochemical systems Chiyang,” *Chin. J. Catal.* **43**, 2858 (2022).
- 7 Y. Ye and Z. Liu, “APXPS of solid/liquid interfaces,” *ACS Symp. Ser.* **1396**, 67–92 (2021).
- 8 M. Favaro, B. Jeong, P. N. Ross, J. Yano, Z. Hussain, Z. Liu, and E. J. Crumlin, “Unravelling the electrochemical double layer by direct probing of the solid/liquid interface,” *Nat. Commun.* **7**, 12695–12698 (2016).

- <sup>9</sup>A. Shavorskiy, X. Ye, O. Karshoğlu, A. D. Poletayev, M. Hartl, I. Zegkinoglou, L. Trotochaud, S. Nemšák, C. M. Schneider, E. J. Crumlin, S. Axnanda, Z. Liu, P. N. Ross, W. Chueh, and H. Bluhm, "Direct mapping of band positions in doped and undoped hematite during photoelectrochemical water splitting," *J. Phys. Chem. Lett.* **8**, 5579–5586 (2017).
- <sup>10</sup>I. Källquist, F. Lindgren, M.-T. Lee, A. Shavorskiy, K. Edström, H. Rensmo, L. Nyholm, J. Maibach, and M. Hahlin, "Probing electrochemical potential differences over the solid/liquid interface in Li-ion battery model systems," *ACS Appl. Mater. Interfaces* **13**, 32989–32996 (2021).
- <sup>11</sup>I. Källquist, T. Ericson, F. Lindgren, H. Chen, A. Shavorskiy, J. Maibach, and M. Hahlin, "Potentials in Li-ion batteries probed by operando ambient pressure photoelectron spectroscopy," *ACS Appl. Mater. Interfaces* **14**, 6465–6475 (2022).
- <sup>12</sup>Y. Zhai, Z. Zhu, S. Zhou, C. Zhu, and S. Dong, "Recent advances in spectroelectrochemistry," *Nanoscale* **10**, 3089–3111 (2018).
- <sup>13</sup>C. S. Ponseca, P. Chábera, J. Uhlig, P. Persson, and V. Sundström, "Ultrafast electron dynamics in solar energy conversion," *Chem. Rev.* **117**, 10940–11024 (2017).
- <sup>14</sup>R. H. Temperton, M. Guo, G. D'Acunto, N. Johansson, N. W. Rosemann, O. Prakash, K. Wärnmark, J. Schnadt, J. Uhlig, and P. Persson, "Resonant x-ray photo-oxidation of light-harvesting iron (II/III) N-heterocyclic carbene complexes," *Sci. Rep.* **11**, 22144 (2021).
- <sup>15</sup>R. H. Temperton, N. W. Rosemann, M. Guo, N. Johansson, L. A. Fredin, O. Prakash, K. Wärnmark, K. Handrup, J. Uhlig, J. Schnadt, and P. Persson, "Site-selective orbital interactions in an ultrathin iron-carbene photosensitizer film," *J. Phys. Chem. A* **124**, 1603–1609 (2020).
- <sup>16</sup>R. H. Temperton, S. T. Skowron, K. Handrup, A. J. Gibson, A. Nicolaou, N. Jaouen, E. Besley, and J. N. O'Shea, "Resonant inelastic x-ray scattering of a Ru photosensitizer: Insights from individual ligands to the electronic structure of the complete molecule," *J. Chem. Phys.* **151**, 074701 (2019).
- <sup>17</sup>S. K. Eriksson, M. Hahlin, S. Axnanda, E. Crumlin, R. Wilks, M. Odelius, A. I. K. Eriksson, Z. Liu, J. Åhlund, A. Hagfeldt, D. E. Starr, M. Bär, H. Rensmo, and H. Siegbahn, "In-situ probing of H<sub>2</sub>O effects on a Ru-complex adsorbed on TiO<sub>2</sub> using ambient pressure photoelectron spectroscopy," *Top. Catal.* **59**, 583–590 (2016).
- <sup>18</sup>A. J. Gibson, R. H. Temperton, K. Handrup, M. Weston, L. C. Mayor, and J. N. O'Shea, "Charge transfer from an adsorbed ruthenium-based photosensitizer through an ultra-thin aluminium oxide layer and into a metallic substrate," *J. Chem. Phys.* **140**, 234708 (2014).
- <sup>19</sup>L. C. Mayor, J. Ben Taylor, G. Magnano, A. Rienzo, C. J. Satterley, J. N. O'Shea, and J. Schnadt, "Photoemission, resonant photoemission, and x-ray absorption of a Ru(II) complex adsorbed on rutile TiO<sub>2</sub>(110) prepared by *in situ* electrospray deposition," *J. Chem. Phys.* **129**, 114701 (2008).
- <sup>20</sup>E. M. J. Johansson, M. Hedlund, M. Odelius, H. Siegbahn, and H. Rensmo, "Frontier electronic structures of Ru(tcterpy)(NCS)<sub>3</sub> and Ru(dcbpy)<sub>2</sub>(NCS)<sub>2</sub>: A photoelectron spectroscopy study," *J. Chem. Phys.* **126**, 244303 (2007).
- <sup>21</sup>R. H. Temperton, W. Quevedo, R. Seidel, J. Uhlig, J. Schnadt, and P. Persson, "Spin propensity in resonant photoemission of transition metal complexes," *J. Chem. Phys.* **3**, 033030 (2021).
- <sup>22</sup>R. Seidel, S. Thürmer, J. Moens, P. Geerlings, J. Blumberger, and B. Winter, "Valence photoemission spectra of aqueous Fe(2<sup>+</sup>/3<sup>+</sup>) and [Fe(CN)<sub>6</sub>]<sup>4-3-</sup> and their interpretation by DFT calculations," *J. Phys. Chem. B* **115**, 11671–11677 (2011).
- <sup>23</sup>S. J. Gerber and E. Erasmus, "Electronic effects of metal hexacyanoferrates: An XPS and FTIR study," *Mater. Chem. Phys.* **203**, 73–81 (2018).
- <sup>24</sup>A. N. Mansour, J. K. Ko, G. H. Waller, C. A. Martin, C. Zhang, X. Qiao, Y. Wang, X. Zhou, and M. Balasubramanian, "Structural analysis of K<sub>4</sub>Fe(CN)<sub>6</sub>·3H<sub>2</sub>O, K<sub>3</sub>Fe(CN)<sub>6</sub> and Prussian Blue," *ECS J. Solid State Sci. Technol.* **10**, 103002 (2021).
- <sup>25</sup>M. Risch, K. A. Stoerzinger, T. Z. Regier, D. Peak, S. Y. Sayed, and Y. Shao-Horn, "Reversibility of ferri-/ferrocyanide redox during operando soft x-ray spectroscopy," *J. Phys. Chem. C* **119**, 18903–18910 (2015).
- <sup>26</sup>R. Seidel, M. N. Pohl, H. Ali, B. Winter, and E. F. Aziz, "Advances in liquid phase soft-x-ray photoemission spectroscopy: A new experimental setup at BESSY II," *Rev. Sci. Instrum.* **88**, 073107 (2017).
- <sup>27</sup>T. Kachel, "The plane grating monochromator beamline U49-2 PGM-1 at BESSY II," *J. Large-Scale Res. Facil. JLSRF* **2**, A72 (2016).
- <sup>28</sup>M. F. Lichterman, S. Hu, M. H. Richter, E. J. Crumlin, S. Axnanda, M. Favaro, W. Drisdell, Z. Hussain, T. Mayer, B. S. Brunshwig, N. S. Lewis, Z. Liu, and H.-J. Lewerenz, "Direct observation of the energetics at a semiconductor/liquid junction by *operando* x-ray photoelectron spectroscopy," *Energy Environ. Sci.* **8**, 2409–2416 (2015).
- <sup>29</sup>C. Ma, S. Pei, and S. You, "Closed bipolar electrode for decoupled electrochemical water decontamination and hydrogen recovery," *Electrochem. Commun.* **109**, 106611 (2019).
- <sup>30</sup>S. W. Boettcher, S. Z. Oener, M. C. Lonergan, Y. Surendranath, S. Ardo, C. Brozek, and P. A. Kempler, "Potentially confusing: Potentials in electrochemistry," *ACS Energy Lett.* **6**, 261–266 (2021).
- <sup>31</sup>I. Källquist, "Combining electrochemistry and photoelectron spectroscopy for the study of Li-ion batteries," Ph.D. thesis, Uppsala University, 2021.
- <sup>32</sup>N. Ottosson, K. J. Børve, D. Spångberg, H. Bergersen, L. J. Sæthre, M. Faubel, W. Pokapanich, G. Öhrwall, O. Björneholm, and B. Winter, "On the origins of core-electron chemical shifts of small biomolecules in aqueous solution: Insights from photoemission and *ab initio* calculations of glycine<sub>aq</sub>," *J. Am. Chem. Soc.* **133**, 3120–3130 (2011).